

# Tunable scaling behaviour observed in Barkhausen criticality of a ferromagnetic film

KWANG-SU RYU<sup>1</sup>, HIRO AKINAGA<sup>2</sup> AND SUNG-CHUL SHIN<sup>1\*</sup>

<sup>1</sup>Department of Physics and Center for Nanospinics of Spintronic Materials, Korea Advanced Institute of Science and Technology, Daejeon 305-701, Korea

<sup>2</sup>Nanotechnology Research Institute, National Institute of Advanced Industrial Science and Technology, 1-1-1 Higashi, Tsukuba, Ibaraki 305-8562, Japan

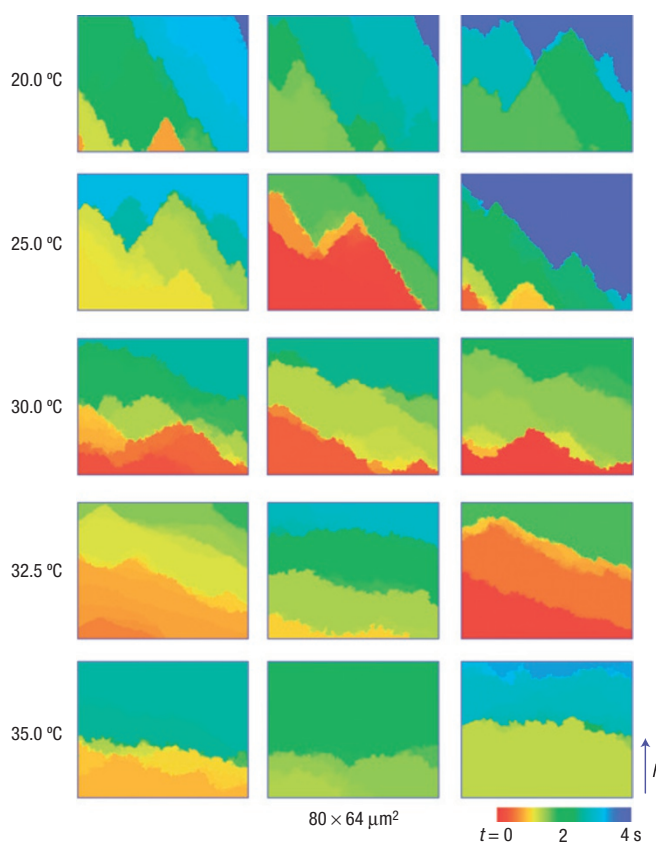
\*e-mail: scshin@kaist.ac.kr

Published online: 15 July 2007; doi:10.1038/nphys659

A ferromagnetic material shows a sequence of discrete and jerky domain jumps, known as the Barkhausen avalanche<sup>1,2</sup>, in the presence of an external magnetic field. Studies of Barkhausen avalanches reveal power-law scaling behaviour that suggests an underlying criticality<sup>3–8</sup>, as observed in a wide variety of systems such as superconductor vortices<sup>9</sup>, microfractures<sup>10</sup>, earthquakes<sup>11</sup>, lung inflations<sup>12</sup>, mass extinctions<sup>13</sup>, financial markets<sup>14</sup> and charge-density waves<sup>15</sup>. The most interesting unsolved fundamental question is whether the universality in the scaling exponent holds regardless of the material and its detailed microstructure. Here we show that the scaling behaviour of Barkhausen criticality in a given ferromagnetic film is experimentally tunable by varying the temperature (not dimensionality). We observe for the first time that the scaling behaviour in the Barkhausen criticality of a given system crosses over between two universality classes when the relative contributions from the dipolar interaction and domain-wall energies are altered by an experimental parameter.

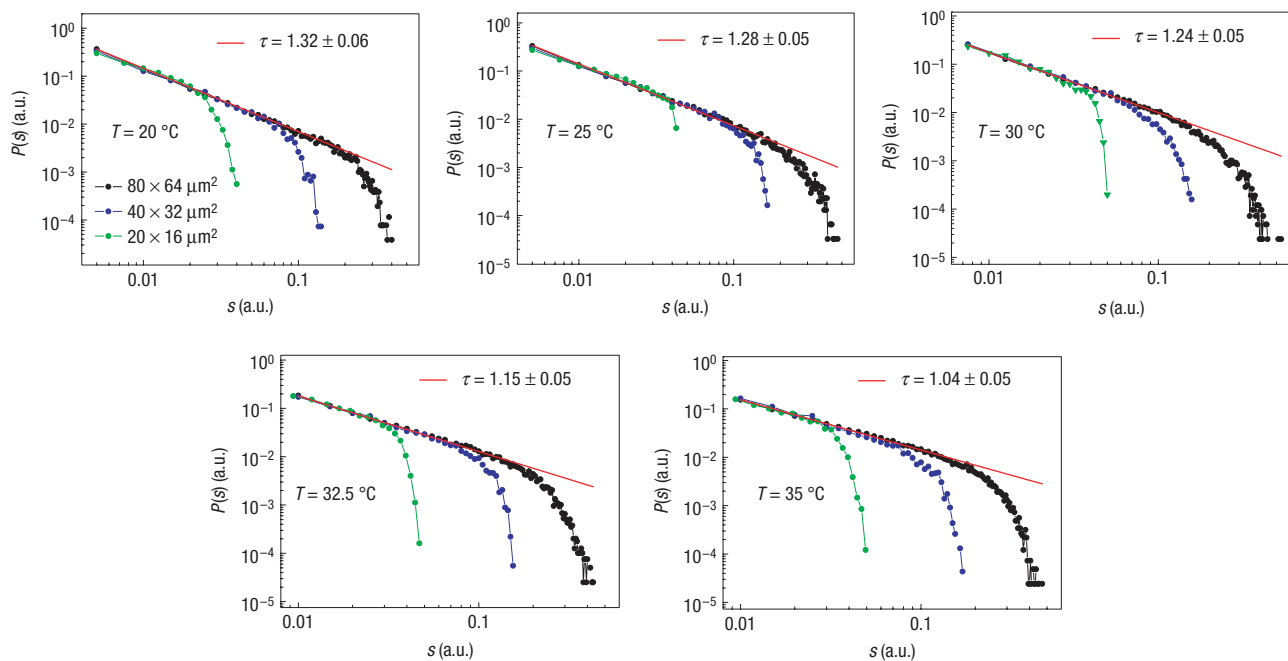
All theoretical works so far predict that the universality of the scaling exponent depends only on the dimensionality of a system, even though the value of the scaling exponent varies according to the theory<sup>16–22</sup>. However, the measured scaling exponents reported in the literature span a relatively wide range of values despite the same dimensionality<sup>3–8</sup>. Thus, the universality has been questioned, and our understanding is far from complete. To test the validity of the universality of Barkhausen criticality, a desirable approach is to make systematic measurements of the scaling exponent under well-controlled experimental conditions with reliable statistics in a given system while maintaining the same dimensionality. A ferromagnetic (FM) MnAs film on GaAs(001) substrate is considered an ideal system for such purposes: it reveals a systematic variation of domain-evolution patterns with temperature during a Barkhausen avalanche, a variation that results from the decrease in the saturation magnetization  $M_S$  with temperature<sup>23</sup>. Thus, scaling behaviour in different domain-evolution patterns in a given system can be investigated in an experimentally controllable manner.

Figure 1 shows representative domain-evolution patterns of the 50 nm MnAs film observed three consecutive times by means of a magneto-optical microscope magnetometer (MOMM) at each designated temperature in a range of 20–35 °C. In Fig. 1, we can clearly see that the domain evolution patterns at each temperature show a sequence of discrete and jerky domain jumps during the magnetization reversal. Also, we found that the domain jumps proceed with randomness of interval, size and location for the repeated experiments, as clearly seen from the three representative domain images at each temperature. From this evidence, it



**Figure 1** Representative domain-evolution patterns at several temperatures in the temperature range of 20–35 °C. These patterns were directly observed with an MOMM on precisely the same area of the MnAs film. Three domain-evolution patterns at each temperature were obtained from repeated experiments. The sample was initially saturated, and a constant field  $H$  was then applied in the opposite direction, as denoted by the solid arrow. Note that 180° domain walls exist throughout the reversal process, which is expected from the uniaxial anisotropy, with an easy axis along the MnAs[1120].

can be concluded that the domain jumps at each temperature correspond to the Barkhausen avalanches in a critical state. The randomness in the locations of the Barkhausen avalanches implies that the disorders in this system are strongly localized and



**Figure 2** The distributions of the Barkhausen avalanche sizes at several temperatures ranging from 20 to 35 °C. Each distribution was obtained through a statistical analysis of the fluctuating size of the Barkhausen jump from experiments carried out more than 1,000 times at each temperature. The avalanche size  $s$  is defined as the area of one jump determined from the domain-area curve with time, corresponding to the time-resolved domain-evolution patterns shown in Fig. 1.

randomly distributed, characteristic of a system showing critical scaling behaviour<sup>5,8</sup>.

An interesting feature related to the Barkhausen criticality of the MnAs film is the systematic variation of the domain-evolution patterns with temperature: a saw-tooth domain-wall structure shows a saw-tooth angle that increases with temperature. Generally, a saw-tooth domain shape develops to reduce the magnetic charge density when two opposite domains meet head on in an FM film with a uniaxial anisotropy<sup>24</sup>. When the angle between the magnetization direction and the easy axis is small because of a strong uniaxial anisotropy, as revealed in the film here, the saw-tooth angle  $2\phi$  is approximated as  $2\phi = \gamma_w/4M_s^2 t$ , that is, the relative magnitude between the domain-wall energy of  $\gamma_w = \pi(A_{\text{ex}}K_{\perp})^{1/2}$  and the dipolar interaction energy of  $4M_s^2$ , where  $A_{\text{ex}}$  is the exchange stiffness,  $K_{\perp}$  is an anisotropy constant in the normal-to-film plane and  $t$  is the sample thickness<sup>23,24</sup>. As already pointed out in ref. 23, the increased saw-tooth angle with increased temperature is mainly attributable to decreased dipolar interaction energy caused by the decrease of  $M_s$  with temperature. Therefore, domain-evolution patterns with a small saw-tooth angle of 60.1° at 20 °C develop to reduce the dipolar interaction energy that results from a larger  $M_s$ ; however, the nearly 180° flat domain walls at 35 °C are formed primarily to minimize the domain-wall area, as the dipolar interaction is negligible owing to a smaller  $M_s$ .

As shown in Fig. 2, the distribution of the Barkhausen avalanche sizes shows power-law scaling behaviour at all temperatures from 20 to 35 °C. In addition, the scaling exponent at each temperature has a constant value, irrespective of the size of the field of view from  $20 \times 16$  to  $80 \times 64 \mu\text{m}^2$ . This finding indicates that the observation is in a critical state, as shown by the critical scaling behaviour. It should be noted that an accurate determination of the scaling exponents, which is very important in the present study, is possible because of the direct visualization of the Barkhausen avalanches using an MOMEM capable of real-time

direct domain observation<sup>8,25</sup>. In Fig. 2, note that a cutoff, at which the distribution deviates from the power-law scaling, exists at all temperatures. Many different effects, including a variation of the disorder distribution<sup>19</sup>, a demagnetization effect<sup>5,6</sup> or a finite-size effect<sup>16,17</sup>, have been suggested as explanations for the origin of the cutoff. Because the cutoff size at each temperature is strongly dependent on the size of the field of view, as clearly seen in Fig. 2, we believe that the cutoff in the power-law distribution of the present system originates from the finite-size effect of the field of view.

The most striking finding in the power-law distribution of the MnAs film is that the scaling exponent varies continuously from 1.32 to 1.04 as the temperature increases, as shown in Fig. 3a. This result suggests that the Barkhausen avalanche at each temperature has a distinctive scaling exponent, which yields a different critical scaling behaviour. We confirmed with thermal cycles that the variation of the scaling exponent is reproducible within the experimental error ranges. This report is the first to show that the scaling exponent of the Barkhausen criticality in a given FM system can be tuned in a controllable manner.

We interpret our experimental data as a crossover scaling behaviour between two universality classes, which is caused by competition between the long-range dipolar interaction and the short-range domain-wall surface tension. Generally, the equation of motion for the domain wall in an FM system with uniaxial in-plane anisotropy is expressed as the sum of the different contributions of the magnetostatic energy, dipolar interaction energy, domain-wall energy and pinning potentials by disorder<sup>5,21</sup>. Using the mean-field approximation and renormalization-group method in the equation, the interaction kernel of an interface in the momentum space can be expressed by a linear combination of the two contributions from the dipolar interaction  $(M_s^2/\pi)|q|$  and the domain-wall surface tension  $\gamma_w q^2$  as follows:

$$J(q) = (M_s^2/\pi)|q| + \gamma_w q^2.$$

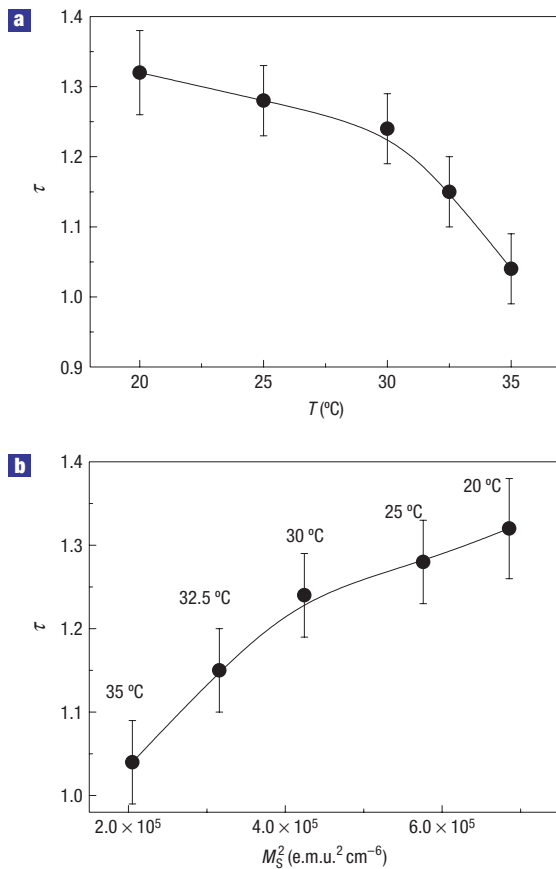


**Figure 3** The experimental values of the scaling exponent  $\tau$ . **a**, The scaling exponent with temperature  $T$  in the temperature range of 20–35 °C. **b**, The scaling exponent as a function of  $M_s^2$ . The saturation magnetization as a function of temperature was measured by a SQUID magnetometer. We define the error bar of the scaling exponent as a difference between maximum and minimum slopes in Fig. 2.

For small  $|q|$  or large  $M_s^2$ , the long-range dipolar interaction is dominant and the interaction kernel in the momentum space is approximated as  $J(q) \propto |q|$ , which predicts a class with a critical exponent of  $\tau = 4/3$  (ref. 22). A similar value of the critical exponent was predicted for the charged zigzag domain wall<sup>26</sup>. On the other hand, for large  $|q|$  or small  $M_s^2$ , the short-range domain-wall surface tension is dominant and the interaction kernel is described by  $J(q) \propto q^2$ , in which a class with the critical exponent of  $\tau = 1$  is predicted, as observed in general elastic interfaces<sup>15,27</sup>. Therefore, it could be interpreted that the scaling exponent continuously varying from 1.32 to 1.04 in the Barkhausen criticality of the MnAs film may be ascribed to a crossover scaling behaviour from the long-range dipolar interaction to the short-range domain-wall surface tension, caused by a decreasing variation of  $M_s^2$  with increasing  $T$  as shown in Fig. 3b. The interpretation that the dominant contribution to the scaling behaviour changes from the dipolar interaction energy to the domain-wall energy with increasing temperature is consistent with the change of the saw-tooth angle in the domain-wall structure, as illustrated in Fig. 1. An increase in the saw-tooth angle with increasing temperature reflects the relative decrease in the contribution of the dipolar interaction compared with the domain-wall contribution.

To extract the universal crossover function between two classes, we have carried out a collapse of  $P(s, T)$  data at

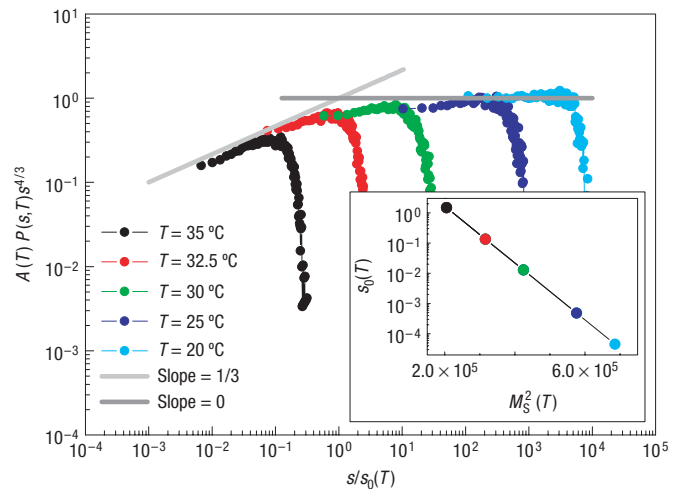


**Figure 4** The collapse of  $P(s, T)$  data at different temperatures.

$A(T)P(s, T)s^{4/3}$  was plotted as a function of  $s/s_0(T)$  in a log–log scale, where  $A(T)$  and  $s_0(T)$  are smooth functions of  $M_s(T)$ . The crossover size  $s_0(T)$  is selected as a decreasing function of  $M_s^2$  as shown in the inset, because our crossover scaling behaviour is mainly ascribed to the change of dipolar interaction energy. The scaling form we use to collapse the data assumes that the size of the field of view is infinite. An experiment in a much larger field of view is expected to capture the entire crossover in one experiment.

different temperatures. Figure 4 shows a plot of  $\log(A(T)P(s, T)s^{4/3})$  versus  $\log(s/s_0(T))$ . Considering the fact that the crossover scaling behaviour in the present system is mainly ascribed to the change of dipolar interaction energy, we take the crossover size  $s_0(T)$  as a decreasing function of  $M_s^2$  expressed by  $\log(s_0(T)) = -(9.4 \times 10^{-6})M_s^2 + (2.1)$ , as shown in the inset. Also, we take  $A(T)$  as a smooth function of  $M_s(T)$  given by  $(1.0 \times 10^{-2})M_s^2 - (5.0)M_s + (6.9 \times 10^2)$ . As shown in this plot, we find a single curved line, where the line starts out with zero slope at large size and low temperature of 20 °C, and ends up with a slope of one-third at small size and high temperature of 35 °C with variation of temperature. Hence, we clearly see a crossover scaling behaviour from a class with the critical exponent of  $\tau = 4/3$ , where the long-range dipolar interaction is dominant, to a class with the critical exponent of  $\tau = 1$ , where the short-range domain-wall surface tension is dominant.

Much of the critical behaviour observed in nature can be explained by the interaction ranges of the interface with only integer values of  $\mu$ , where the interaction kernel of the interface is generalized as  $J(q) \propto |q|^\mu$ . For example, the dipolar interaction in an FM system<sup>5,6</sup> and the contact line<sup>28</sup> correspond to critical behaviours with  $\mu = 1$ . On the other hand, critical behaviour with  $\mu = 2$  is generated from the general elastic interfaces such as the domain-wall energy in an FM system<sup>5,6</sup> and charge-density waves<sup>15,27</sup>. Thus, two universality classes characterized by the interaction range  $\mu$  with an integer value are used to understand the critical behaviour. However, the present work demonstrates that a universal crossover behaviour between two different critical points ( $\mu = 1$  and  $\mu = 2$ ) appears when two interactions of the interface with different interaction ranges compete in a system.

## METHODS

### EXPERIMENTAL SAMPLE

A MnAs film 50 nm thick was epitaxially grown on GaAs(001) substrate at 270 °C by molecular-beam epitaxy. The epitaxial relationship in the

film plane was  $\text{MnAs}(\bar{1}100) \parallel \text{GaAs}(001)$ ,  $\text{MnAs}[0001] \parallel \text{GaAs}[\bar{1}10]$ , and  $\text{MnAs}[1120] \parallel \text{GaAs}[110]$ . From the torque and vibrating sample magnetometric measurements, the sample was found to have an in-plane magnetic anisotropy with an easy axis along the  $\text{MnAs}[\bar{1}120]$ , a hard axis along  $\text{MnAs}[0001]$ , and an intermediate axis for the out-of-plane direction along  $\text{MnAs}[\bar{1}100]$ . Atomic force and magnetic force microscopy studies of the  $\text{MnAs}$  film revealed that the hexagonal FM  $\alpha$ - $\text{MnAs}$  and non-FM orthorhombic  $\beta$ - $\text{MnAs}$  stripes were intercalated with each other along  $\text{MnAs}[0001]$  via strain stabilization, lying perpendicular to a magnetic easy axis along  $\text{MnAs}[\bar{1}120]$  (ref. 29). The variation of the saturation magnetization  $M_S$  with temperature was measured using a superconductor quantum interference device (SQUID) magnetometer, and the value of  $M_S$  was found to decrease as temperature increased. The decrease of  $M_S$  with increasing temperature is ascribed mainly to the decrease of the FM  $\alpha$ - $\text{MnAs}$  volume ratio according to temperature, as confirmed by a temperature-dependent X-ray diffraction experiment.

#### MEASUREMENT OF BARKHAUSEN AVALANCHES

Barkhausen avalanche of the  $\text{MnAs}$  film at criticality was directly observed on a  $80 \times 64\text{-}\mu\text{m}^2$  sample area by means of MOMM, capable of real-time direct domain observation<sup>8,25</sup>. The MOMM system basically consists of a polarizing optical microscope, which can visualize magnetic contrast via a longitudinal magneto-optical Kerr effect. The spatial resolution is 400 nm at  $\times 500$  magnification, and the system is equipped with an advanced video processing set with an image-grabbing rate of 30 frames  $\text{s}^{-1}$  in real time. The Barkhausen avalanche was triggered by applying approximately 99% of the coercive field to an initially saturated sample. The sample could be heated to a maximum of 80 °C using a heater placed at the sample stage for the temperature-dependent study. The Barkhausen jump was directly visualized and characterized from serial time-resolved domain images taken at various temperatures.

Received 13 February 2007; accepted 5 June 2007; published 15 July 2007.

#### References

- Barkhausen, H. *Zwie mit hilfe der neuen verstärkter entdeckte erscheinungen*. *Phys. Z.* **20**, 401–403 (1919).
- Durin, G. & Zapperi, S. in *The Science of Hysteresis* (eds Bertotti, G. & Mayergoyz, I.) 181–267 (Academic, New York, 2005).
- Urbach, J. S., Madison, R. C. & Markert, J. T. Interface depinning, self-organized criticality, and the Barkhausen effect. *Phys. Rev. Lett.* **75**, 276–279 (1995).
- Spasojevic, D., Bukvic, S., Milosevic, S. & Stanley, H. E. Barkhausen noise: Elementary signals, power laws, and scaling relations. *Phys. Rev. E* **54**, 2531–2546 (1996).
- Zapperi, S., Cizeau, P., Durin, G. & Stanley, H. E. Dynamics of a ferromagnetic domain wall: Avalanches, depinning transition, and the Barkhausen effect. *Phys. Rev. B* **58**, 6353–6366 (1998).
- Durin, G. & Zapperi, S. Scaling exponents for Barkhausen avalanches in polycrystalline and amorphous ferromagnets. *Phys. Rev. Lett.* **84**, 4705–4708 (2000).
- Puppini, E. Statistical properties of Barkhausen noise in thin Fe films. *Phys. Rev. Lett.* **84**, 5415–5418 (2000).
- Kim, D.-H., Choe, S.-B. & Shin, S.-C. Direct observation of Barkhausen avalanche in Co thin films. *Phys. Rev. Lett.* **90**, 087203 (2003).
- Field, S., Witt, J., Nori, F. & Ling, X. Superconducting vortex avalanches. *Phys. Rev. Lett.* **74**, 1206–1209 (1995).
- Zapperi, S., Vespignani, A. & Stanley, H. E. Plasticity and avalanche behaviour in microfracturing phenomena. *Nature* **388**, 658–660 (1997).
- Sethna, J. P., Dahmen, K. A. & Myers, C. R. Crackling noise. *Nature* **410**, 242–250 (2001).
- Suki, B., Barabási, A.-L., Hantos, Z., Peták, F. & Stanley, H. E. Avalanches and power-law behaviour in lung inflation. *Nature* **368**, 615–618 (1994).
- Solé, R. V., Manrubia, S. C., Benton, M. & Bak, P. Self-similarity of extinction statistics in the fossil record. *Nature* **388**, 764–767 (1997).
- Lux, T. & Marchesi, M. Scaling and criticality in a stochastic multi-agent model of a financial market. *Nature* **397**, 498–500 (1999).
- Fisher, D. S. Threshold behavior of charge-density waves pinned by impurities. *Phys. Rev. Lett.* **50**, 1486–1489 (1983).
- Bak, P., Tang, C. & Wiesenfeld, K. Self-organized criticality: An explanation of 1/f noise. *Phys. Rev. Lett.* **59**, 381–384 (1987).
- Cote, P. J. & Meisel, L. V. Self-organized criticality and the Barkhausen effect. *Phys. Rev. Lett.* **67**, 1334–1337 (1991).
- Sethna, J. P. *et al.* Hysteresis and hierarchies: Dynamics of disorder-driven first-order phase transformations. *Phys. Rev. Lett.* **70**, 3347–3350 (1993).
- Perković, O., Dahmen, K. & Sethna, J. P. Avalanches, Barkhausen noise, and plain old criticality. *Phys. Rev. Lett.* **75**, 4528–4531 (1995).
- Narayan, O. Self-similar Barkhausen noise in magnetic domain wall motion. *Phys. Rev. Lett.* **77**, 3855–3857 (1996).
- Cizeau, P., Zapperi, S., Durin, G. & Stanley, H. E. Dynamics of a ferromagnetic domain wall and the Barkhausen effect. *Phys. Rev. Lett.* **79**, 4669–4672 (1997).
- Vázquez, O. & Sotolongo-Costa, O. Dynamics of a domain wall in soft-magnetic materials: Barkhausen effect and relation with sandpile models. *Phys. Rev. Lett.* **84**, 1316–1319 (2000).
- Ryu, K.-S., Shin, S.-C., Akinaga, H. & Manago, T. Real-time direct observation of temperature-dependent domain reversal behavior in epitaxial  $\text{MnAs}$  film on  $\text{GaAs}(001)$ . *Appl. Phys. Lett.* **88**, 122509 (2006).
- Ryu, K.-S., Kim, D.-H., Shin, S.-C. & Akinaga, H. Real-time direct observation of asymmetric magnetization reversal in exchange-biased single-layer systems. *Phys. Rev. B* **71**, 155308 (2005).
- Choe, S.-B. *et al.* Magneto-optical microscope magnetometer for simultaneous local probing of magnetic properties. *Rev. Sci. Instrum.* **73**, 2910–2916 (2002).
- Cerruti, B. & Zapperi, S. Barkhausen noise from zigzag domain walls. *J. Stat. Mech.* **6**, P08020 (2006).
- Narayan, O. & Fisher, D. S. Threshold critical dynamics of driven interfaces in random media. *Phys. Rev. B* **48**, 7030–7042 (1993).
- Ertas, D. & Kardar, M. Critical dynamics of contact line depinning. *Phys. Rev. E* **49**, R2532–R2535 (1994).
- Plake, T. *et al.* Periodic elastic domains of coexisting phases in epitaxial  $\text{MnAs}$  films on  $\text{GaAs}$ . *Appl. Phys. Lett.* **80**, 2523–2525 (2002).

#### Acknowledgements

The authors would like to express sincere thanks to K.-D. Lee at KAIST for the data analysis, T. Manago at AIST for the sample preparation and H.-C. Kim at KBSI for helping with the SQUID measurements. This work was supported by KOSEF through the Basic Research Program, KAIST through the Leading Basic S&T Research Project and MOST through the Cavendish–KAIST Research Cooperation Project. Correspondence and requests for materials should be addressed to S.-C.S.

#### Author contributions

K.-S.R. and S.-C.S. contributed to experimental work and data analysis and H.A. contributed to sample preparation.

#### Competing financial interests

The authors declare no competing financial interests.

Reprints and permission information is available online at <http://npg.nature.com/reprintsandpermissions/>